NAVARO II, A new parallel robot with eight actuation modes

Damien Chablat, Luc Rolland

Proceedings of the ASME 2018 International Design Engineering Technical Conferences & Computers and Information in Engineering Conference
IDETC/CIE 2018
August 26-29, , Québec, Canada

DETC2018-85949

NAVARO II, A NEW PARALLEL ROBOT WITH EIGHT ACTUATION MODES

Damien Chablat
CNRS, Laboratoire des Sciences du Numérique de Nantes
UMR CNRS 6004, 1 rue de la Noë,
44321 Nantes
Email: damien.chablat@cnrs.fr

Luc Rolland
School of Engineering and Computing
University of the West of Scotland,
Paisley, Scotland, UK
Email: luc.rolland@uws.ac.uk

ABSTRACT

This article presents a new variable actuation mechanism based on the 3-RPR parallel robot. This mechanism is an evolution of the NaVARo robot, a 3-RRR parallel robot, for which the second revolute joint of the three legs is replaced by a scissor to obtain a larger working space and avoid the use of parallelograms to operate the second revolute joint. To obtain a better spatial rigidity, the leg mechanism is constructed by placing the scissors in an orthogonal plane to the displacement. Unlike the first NaVARO robot, the kinematic model is simpler because there is only one solution to the inverse kinematic model. Surfaces of singularity can be calculated and presented in a compact form. The singularity equations are presented for a robot with a similar base and mobile platform.

INTRODUCTION

A major drawback of serial and parallel mechanisms is the inhomogeneity of kinetostatic performance in their workspace. For example, dexterity, accuracy and stiffness are generally poor in the vicinity of the singularities that may appear in the working space of these mechanisms. For parallel robots, their inverse kinematics problem often has several solutions, which can be called "working mode" [1]. However, it is difficult to achieve a large workspace without singularity for a given working mode. Therefore, it is necessary to plan a change path of the working mode to avoid parallel singularities [2, 3]. In such a case, the initial trajectory would not be followed.

One solution to this problem is to introduce activation redundancy, which involves force control algorithms [4]. Another approach is to use the concept of joint coupling as proposed by [5] or to select the articulation actuated in each leg in relation to the placement of the end-effector, [6], as emphasized in this article.

To solve this problem, a first variable actuation mechanism (VAM) was introduced in 2008 [7], called NaVARo for Nantes Variable Actuation Robot. This mechanism has eight actuation modes and is based on a 3-RRR parallel robot with either the first or second revolute joint actuated. As this mechanism has eight solutions to the inverse kinematic model, the determination of singularities and separation according to the current working mode is very difficult algebraically [8]. In addition, the volume swept by the robot's legs is large and parallelograms reduce the workspace. A framework has been developed to pilot the prototype of this robot. The main problem comes from the position of the position sensor on the motor, which is not always connected to the robot base. Additional sensors may separate assembly modes, but a slight slip in the couplings may disturb the location of the mobile platform [9].

The aim of the article is to propose a new mechanism, based on the 3-RPR parallel robot for which singularities are easier to calculate for all actuation modes. The outline of this article is as follows. The first section presents the architecture of the NaVARo II robot with its eight actuation modes. The second section presents the study of kinematics and presents the algebraic equations of parallel singularities as well as the limits of the workspace. Depending on these limits, the singular surfaces are reduced to present only the singularities in the workspace.

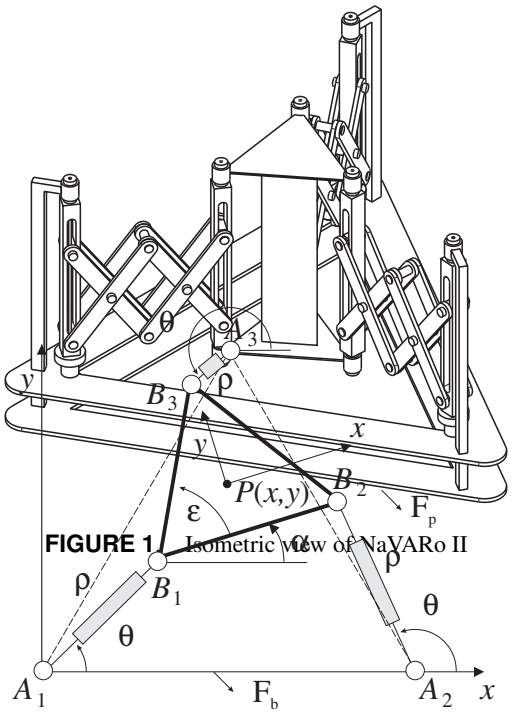

FIGURE 1. Isometric view of NaVARo II

FIGURE 2. 3-RPR with variable actuation

Mechanism architecture of the NaVARo II

The VAM concept was examined in [5, 6]. They derived a VAM from the architecture of the 3-RPR planar parallel manipulator by actuating either the first revolute joint or the prismatic joint of its legs. The same concept was introduced in [7] based on the 3-RRR and a first prototype was created in [10].

The new 3-RPR robot concept with variable actuation is shown in Fig. 1. The use of scissors makes it possible to limit the space requirement during movements in contrast to previous designs and improves rigidity. The number of scissors can be optimized according to the possible height of the mobile platform, the desired stiffness or the desired maximum length of the equivalent prismatic joint [11–13].

This mechanism can be represented on a projection like all 3-RPR mechanisms. The pose of the mobile platform is determined by the Cartesian coordinates (x, y) of the operating point P expressed in the basic frame F_b and the angle α, i.e. the angle between the reference frames F_b and F_p (Figure 2). To illustrate this article, the following dimensions have been fixed, $A_1A_2 = A_1A_3 = A_2A_3 = 90$, $B_1B_2 = B_1B_3 = B_2B_3 = 30$, $\varepsilon = \pi/3$ and $8 \leq \rho_i \leq 59$ for $i = 1,2,3$.

A new transmission system has been developed and installed in each branch of the NaVARo II so that the manipulator can easily switch from one actuation mode to another. As for NaVARo I, it consists of one motor with a shaft connected to two clutches to make the pivot connection between the base and the leg or to

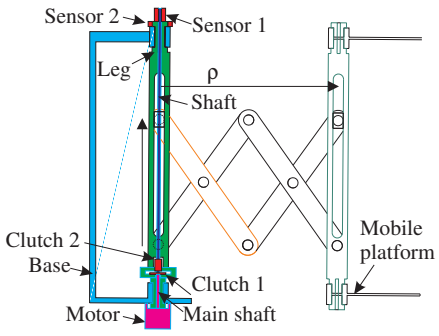

FIGURE 3. The NAVARO II transmission system

make a prismatic joint to operate the scissor. Figure 3 shows a actuation diagram of the NaVARo II. This system can be considered as a double clutch and contains: (i) an electric motor (pink), (ii) a main shaft (pink), (iii) a base (blue), (iv) the first axis of the leg (green), and (v) two electromechanical clutches (red) which connects to the shaft of the first revolute joint (orange) or to the prismatic link shaft (yellow). Two position sensors give the angular position of the leg relative to the base (sensor 1) and the length of the prismatic joint via the ball screw position (sensor 2). The values of the two sensors, combined with the joint limits, allow us to know the current assembly mode of the robot.

The actuation modes are slightly different from the NaVARo I. Each transmission system has four actuation schemes, that are defined thereafter:

1. **None of clutches 1 and 2 are active**. The main shaft can move freely in relation to the base. In this case, neither the pivot joint nor the prismatic joint is actuated. The leg can move freely, i. e. θ_i or ρ_i are passive, $i = 1,2,3$.
2. **Clutch 1 is active while clutch 2 is not**. The first leg axis (green) is driven by the rotation of the motor shaft. In this case, the angle θ_i is active while ρ_i is passive, i = 1,2,3.
3. **Clutch 2 is active while clutch 1 is not**. The first leg joint is free but the rotation of the motor shaft leads to a displacement of the slider, which activates the scissor. In this case, the θ_i is passive and ρ_i is active, $i = 1,2,3$.
4. **Both clutches 1 and 2 are active**. Both joints cause a synchronized rotation and translation motion. The end of the leg will make a spiral motion.

The latter actuation mode differs from the NaVARo I. Only the second and third actuation modes are used in our study. Thus, NaVARo II has eight actuation modes, as shown in Table 1. For example, the first actuation mode corresponds to the 3-RPR mechanism, also referred to as the RPR$_1$-RPR$_2$-RPR$_3$ mechanism, since the first revolute joint (located at point A_i) of its leg are actuated. Similarly, the eighth actuation mode corresponds to the 3-RPR manipulator, also known as the RPR$_1$-RPR$_2$-RPR$_3$ mechanism, since the prismatic joints of its leg are actuated.

TABLE 1. The eight actuating modes of the 3-RRR VAM

Actuating mode number		active joints
1	$\underline{R}PR_1$-$\underline{R}PR_2$-$\underline{R}PR_3$	θ_1, θ_2, θ_3
2	$\underline{R}PR_1$-$\underline{R}PR_2$-$R\underline{P}R_3$	θ_1, θ_2, ρ_3
3	$\underline{R}PR_1$-$R\underline{P}R_2$-$\underline{R}PR_3$	θ_1, ρ_2, θ_3
4	$R\underline{R}P_1$-$\underline{R}PR_2$-$\underline{R}PR_3$	ρ_1, θ_2, θ_3
5	$\underline{R}PR_1$-$R\underline{P}R_2$-$R\underline{P}R_3$	θ_1, ρ_2, ρ_3
6	$R\underline{R}P_1$-$R\underline{P}R_2$-$\underline{R}PR_3$	ρ_1, ρ_2, θ_3
7	$R\underline{P}R_1$-$\underline{R}PR_2$-$R\underline{P}R_3$	ρ_1, θ_2, ρ_3
8	$R\underline{P}R_1$-$R\underline{P}R_2$-$R\underline{P}R_3$	ρ_1, ρ_2, ρ_3

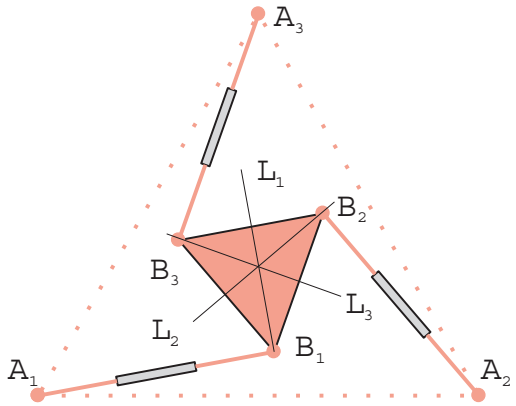

FIGURE 4. Example of singular configuration for the first actuation mode when the lines L_1, L_2 and L_3 intersect at one point

Kinematic modeling of the NaVARo II

In this section, we present the kinematic model that is commonly used to define geometrically singular configurations, then the constraint equations, the workspace boundaries and surfaces that define the singularity loci.

Kinematic modeling

The velocity $\dot{\mathbf{p}}$ of point P can be obtained in three different forms, depending on which leg is traversed, namely,

$$\dot{\mathbf{p}} = \dot{\theta}_i \mathbf{E}(\mathbf{b}_i - \mathbf{a}_i) + \dot{\rho}_i \frac{\mathbf{b}_i - \mathbf{a}_i}{||\mathbf{b}_i - \mathbf{a}_i||} + \dot{\alpha}\mathbf{E}(\mathbf{p} - \mathbf{b}_i) \tag{1}$$

with matrix $\mathbf{E}$ defined as

$$\mathbf{E} = \begin{bmatrix} 0 & -1 \\ 1 & 0 \end{bmatrix} \tag{2}$$

Thus, $\mathbf{p}$, $\mathbf{b}_i$, $\mathbf{a}_i$ are the position vectors of points P, A_i and B_i, respectively, and $\dot{\alpha}$ is the rate of angle α.

To compute the kinematic model, we have to eliminate the idle joints θ_i or ρ_i as a function of the actuation mode. For $\dot{\theta}_i$, we have to dot-multiply by

$$\mathbf{h}_i = (\mathbf{b}_i - \mathbf{a}_i)^T \tag{3}$$

and for $\mathbf{h}_i = \dot{\rho}_i$ by

$$\mathbf{E}\frac{\mathbf{b}_i - \mathbf{a}_i}{||\mathbf{b}_i - \mathbf{a}_i||}. \tag{4}$$

The kinematic model of the VAM can now be cast in vector form, namely,

$$\mathbf{A}\mathbf{t} = \mathbf{B}\dot{\mathbf{q}} \quad \text{with} \quad \mathbf{t} = [\dot{\mathbf{p}} \;\; \dot{\alpha}]^T \quad \text{and} \quad \dot{\mathbf{q}} = [\dot{q}_1 \; \dot{q}_2 \; \dot{q}_3]^T \tag{5}$$

with $\dot{\mathbf{q}}_i$ thus being the vector of actuated joint rates where $\dot{q}_i = \dot{\theta}_i$ when the first revolute joint is driven and $\dot{q}_i = \dot{\rho}_i$ when the prismatic joint is driven, for $i = 1,2,3$. $\mathbf{A}$ and $\mathbf{B}$ are respectively, the direct and the inverse Jacobian matrices of the mechanism, defined as

$$\mathbf{A} = \begin{bmatrix} \mathbf{h}_1 & \mathbf{h}_1\mathbf{E}(\mathbf{p} - \mathbf{b}_1) \\ \mathbf{h}_2 & \mathbf{h}_2\mathbf{E}(\mathbf{p} - \mathbf{b}_2) \\ \mathbf{h}_1 & \mathbf{h}_3\mathbf{E}(\mathbf{p} - \mathbf{b}_3) \end{bmatrix} \tag{6}$$

$$\mathbf{B} = \text{diag}[\rho_1 \; \rho_2 \; \rho_3] \tag{7}$$

The geometric conditions for parallel singularities are well known in the literature for the first and eighth actuation modes. For the first actuation mode, it is when the lines L_i, normal to the axis (A_iB_i) are intersecting at one point, see Fig. 4. For the eighth actuation mode, it is when the lines M_i, passing through the axis (A_iB_i) are intersecting at one point, see Fig. 5. For the other modes, it is just necessary to consider either the L_i or M_i lines according to the actuated joints, i.e. L_i when the i^{th} revolute joint is actuated and M_i when the i^{th} prismatic joint is actuated.

Constraint equations

To maintain the symmetry of the robot, the position of the end-effector is in the center of the mobile platform. The constraint equations for all actuation modes can be written by traversing the closed loops of the mechanism. Equations 8-11

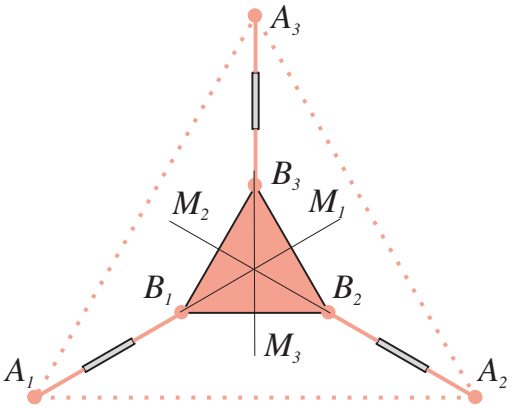

FIGURE 5. Example of singular configuration for the eighth actuation mode when the lines L_1, L_2 and L_3 intersect at one point

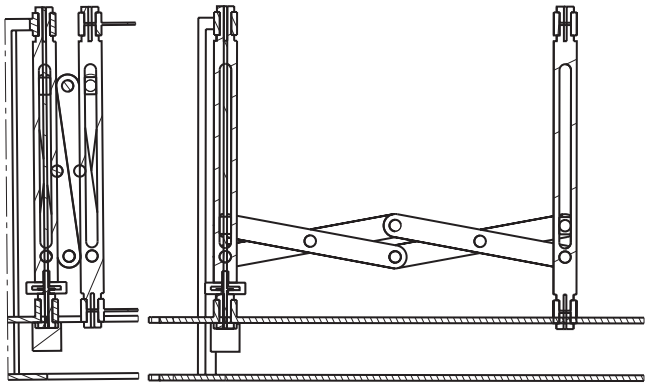

FIGURE 6. Minimum and maximum lengths of the scissors

describe the two closed loops and equations 12-13 define the position and orientation of the mobile platform.

$$\rho_1 C_{\theta_1} + 30C_\alpha - \rho_2 C_{\theta_2} - 90 = 0 \quad (8)$$
$$\rho_1 S_{\theta_1} + 30S_\alpha - \rho_2 S_{\theta_2} = 0 \quad (9)$$
$$\rho_1 C_{\theta_1} + 15(C_\alpha - \sqrt{3}S_\alpha - 3) - \rho_3 C_{\theta_3} = 0 \quad (10)$$
$$\rho_1 S_{\theta_1} + 15(S_\alpha + \sqrt{3}C_\alpha - 3\sqrt{3}) - \rho_3 S_{\theta_3} = 0 \quad (11)$$
$$x - \rho_1 C_{\theta_1} - 15C_\alpha + 5\sqrt{3}S_\alpha = 0 \quad (12)$$
$$y - \rho_1 S_{\theta_1} - 15S_\alpha - 5\sqrt{3}C_\alpha = 0 \quad (13)$$

with $C_\alpha = \cos(\alpha)$, $S_\alpha = \sin(\alpha)$, $C_{\theta_i} = \cos(\theta_i)$, $S_{\theta_i} = \sin(\theta_i)$ for $i = 1,2,3$. To make these equations algebraic, we use a substitution of all trigonometric functions as well as the square root function with

$$\sqrt{3} = S3 \quad \text{and} \quad S3^2 = 3$$
$$\cos(\beta) = C_\beta \quad \text{and} \quad \sin(\beta) = S_\beta \quad \text{for any angles } \beta.$$

We obtain a system with 11 equations, four for loop closures, two for the position and orientation of the mobile platform, four for trigonometric functions and one for the square root function with 14 unknowns. In this case, the manipulation of equations is not trivial and powerful algebraic tools must be used like the Siropa library implemented in Maple [14, 15].

Workspace boundaries

If the revolute joints have no limits, the boundary of the workspace is given by the minimum and maximum extension of the scissors as shown in Fig. 6. The minimum value of ρ_i permits to avoid serial singular configuration where $\rho_i = 0$. Using the constraint equations and ranges limits of prismatic joints ($8 \leq \rho_i \leq 59$), we find six surface equations that describe the boundary of the working space. These limits mean that there is no collision between the legs and the mobile platform.

$$10\sqrt{3}(xS_\alpha - yC_\alpha) + x^2 - 30xC_\alpha + y^2 - 30yS_\alpha - 3181 = 0 \quad (14)$$
$$(-10C_\alpha y + 10S_\alpha(x-90))\sqrt{3} + (30x - 2700)C_\alpha + x^2 + y^2 + 30yS_\alpha - 180x + 4919 = 0 \quad (15)$$
$$(20C_\alpha y + (-20x + 900)S_\alpha - 90y)\sqrt{3} + x^2 + y^2 - 90x - 2700C_\alpha + 4919 = 0 \quad (16)$$
$$10\sqrt{3}(xS_\alpha - yC_\alpha) + x^2 - 30xC_\alpha + y^2 - 30yS_\alpha + 236 = 0 \quad (17)$$
$$(-10C_\alpha y + 10S_\alpha(x-90))\sqrt{3} + (30x - 2700)C_\alpha + x^2 + y^2 + 30yS_\alpha - 180x + 8336 = 0 \quad (18)$$
$$(20C_\alpha y + (-20x + 900)S_\alpha - 90y)\sqrt{3} + x^2 + y^2 - 90x - 2700C_\alpha + 8336 = 0 \quad (19)$$

One of the functions of the Siropa library is to display surfaces that can be limited by inequality equations. The surfaces in blue, red, green represent the minimum and maximum limits of leg one, two and three, respectively in Fig. 7. The projections onto the planes (xy), $(x\alpha)$ and $(y\alpha)$ are used to estimate the main dimensions of the workspace. A cylindrical algebraic decomposition (CAD) can also be performed to have a partition of the workspace for each actuation mode [16].

Singular configurations

From the constraint equations, it is possible to write the determinant of matrix **A**. These determinants depend on the positions of the mobile platform and the positions of the passive and active joints. Only an elimination method like Groebner's basis

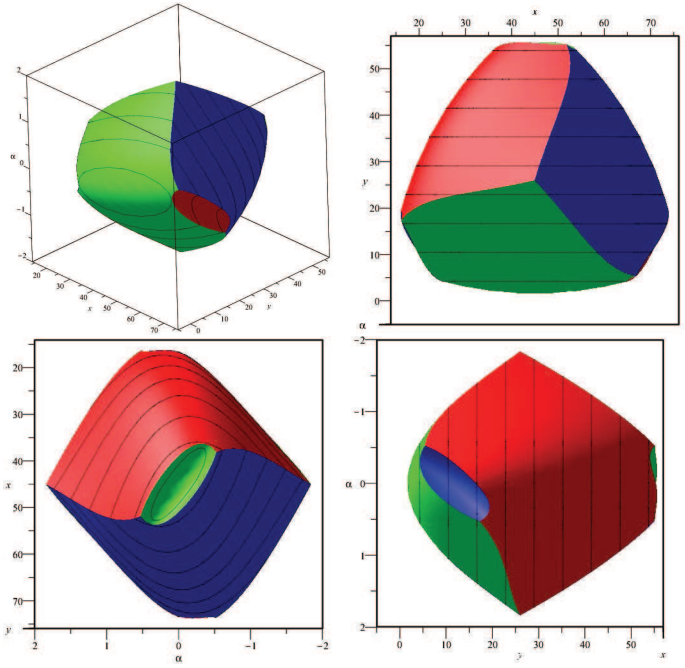

FIGURE 7. Workspace of the NaVARo II in isometric view and three projections onto the planes (xy), $(x\alpha)$ and $(y\alpha)$

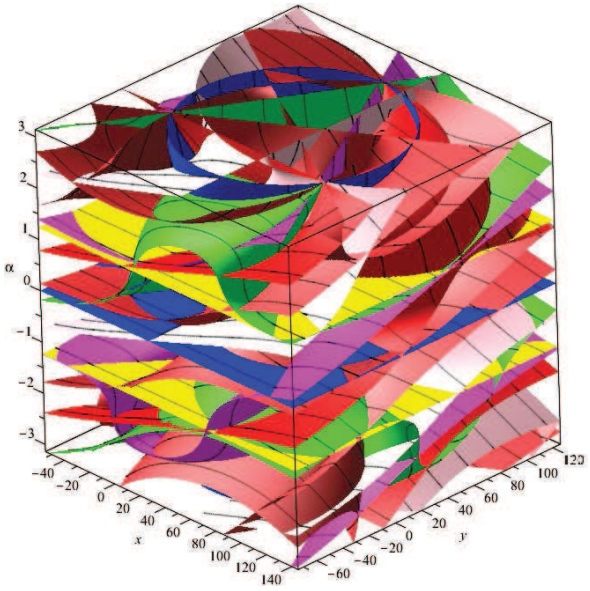

FIGURE 8. The singularity surfaces for the eight actuation modes

can successfully obtain the representation of singularities in the Cartesian workspace. Note that for only the first and eighth actuation modes, the determinant of $\mathbf{A}$ is factorized to form two parallel planes (for the eighth actuation mode, an unrepresented singularity exists for $\alpha = \pi$). The equations of the singularities for the eight actuation modes are given in the Appendix. As there is only one working mode, the equations of these surfaces are simpler than for the NAVARO I robot for which it is not possible to simply describe these equations.

Figures 8 and 9 show all singularities for the eight actuation modes without and with the joint limit conditions. As none of them are superposed, it is possible to completely move through the workspace by choosing a non singular actuation mode for any position of the mobile platform. The same motion planning algorithm introduced for NaVARo I can be used to select the actuation mode able to avoid singular configurations [17].

Figures 10-17 represent the singularities of each actuation mode with on the left the singularities without joint limits and on the right the one included in the workspace. The three actuation modes where a single prismatic joint is actuated are similar by a rotation of 120 degrees (Figs. 11-13). Similarly, the actuation modes where only one revolute joint actuated are also similar (Figs. 14-16).

Conclusions

In this article, a new version of the NaVARo robot was introduced. Thanks to the change of actuation mode, the entire Cartesian workspace can be used. By eliminating the parallelograms that allowed the first NaVARO robot to have an actuation on the second pivot joint, the Cartesian workspace is larger. In addition, it is possible to place sensors on both actuated joints of each leg to locate the mobile platform when we solve the direct kinematic problem. The use of scissors makes it possible to have a greater rigidity in the transverse direction of the robot movement as well as a variation of displacement which can be increased according to the number of bars. Unlike the NaVARo I, which is based on a 3-RRR robot, the NaVARo II is based on the architecture of the 3-RPR, which has only one solution with the inverse kinematic model for any actuation mode. This property allows a complete writing of singularity equations whereas for the robot 3-RRR, in the literature, these equations can be written only for a given orientation of the mobile platform. Future works will be carried out to evaluate the stiffness of the robot based on the size and the number of scissors and the number of solutions to the direct kinematic model to determine if there are actuation modes for which the robot is cuspidal.

REFERENCES

[1] Chablat, D. and Wenger, P., Working Modes and Aspects in Fully-Parallel Manipulator, *Proceeding IEEE International Conference on Robotics and Automation*, pp. 1964–1969,

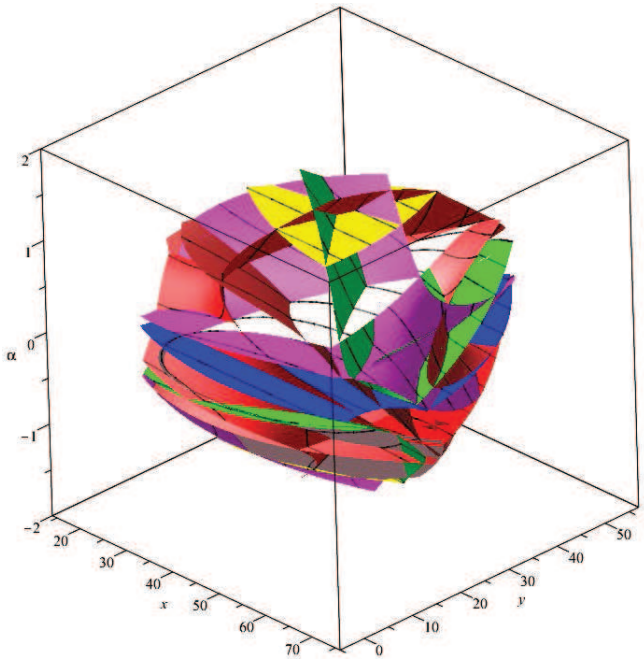

FIGURE 9. The singularity surfaces for the eight actuation modes in the robot workspace

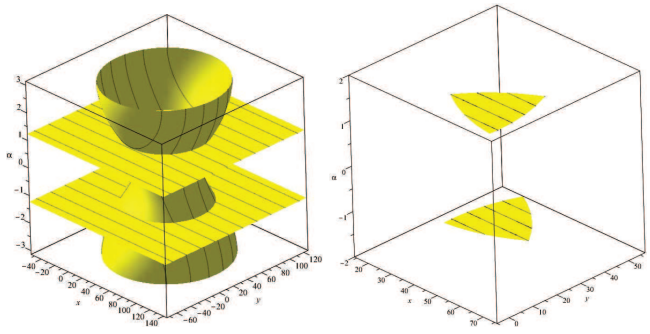

FIGURE 10. Singularity surfaces for actuation modes 1

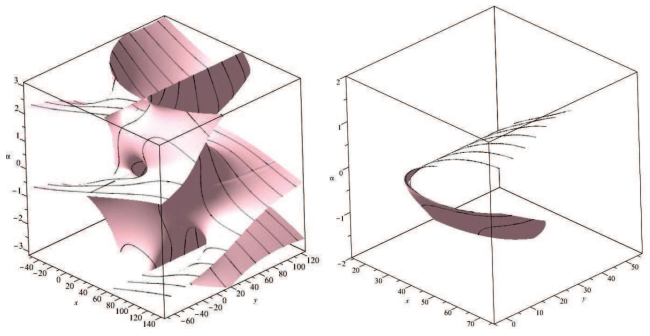

FIGURE 11. Singularity surfaces for actuation modes 2

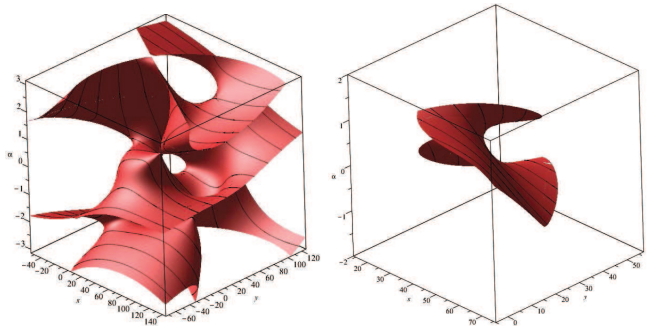

FIGURE 12. Singularity surfaces for actuation modes 3

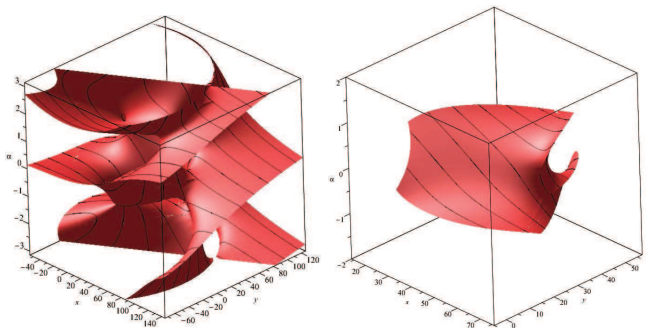

FIGURE 13. Singularity surfaces for actuation modes 4

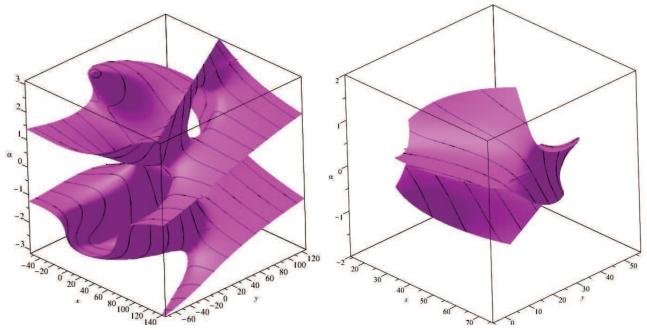

FIGURE 14. Singularity surfaces for actuation modes 5

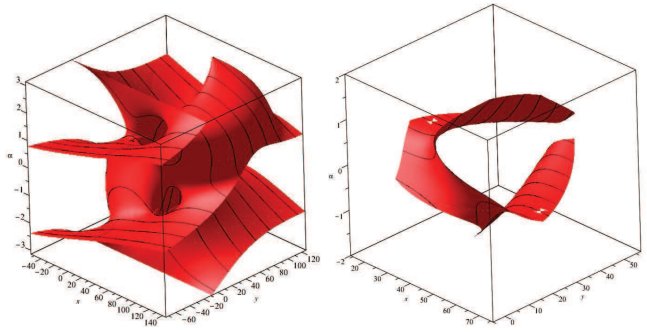

FIGURE 15. Singularity surfaces for actuation modes 6

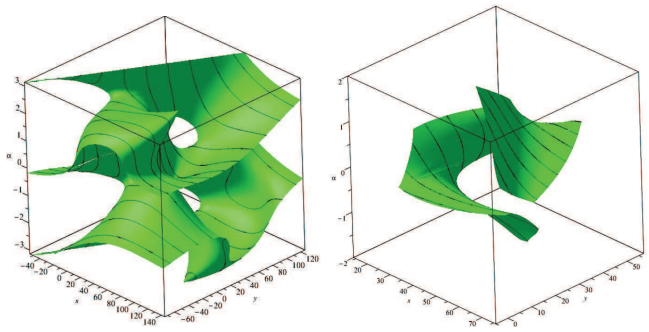

FIGURE 16. Singularity surfaces for actuation modes 7

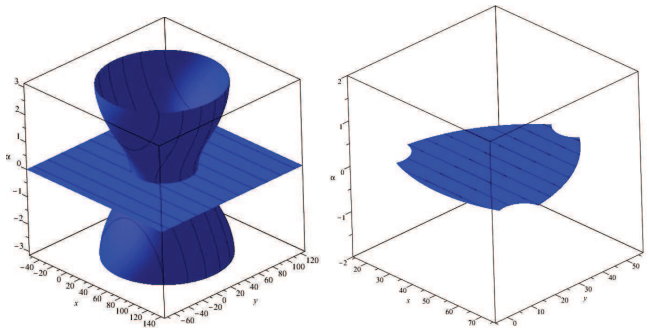

FIGURE 17. Singularity surfaces for actuation modes 8

May, 1998.

[2] Chablat, D. and Wenger, P., Moveability and Collision Analysis for Fully-Parallel Manipulators, *12th CISM-IFTOMM Symposium, RoManSy*, pp. 61-68, Paris, July, 1998

[3] Wenger, P., Chablat, D. Kinematic Analysis of a New Parallel Machine Tool: the Orthoglide, Advances in Robot Kinematics, J. Lenarcic and M. M. Stanisic, eds., Kluwer Academic Publishers, pp. 305-314, 2000.

[4] Alba-Gomez, O., Wenger, P. and Pamanes, A., Consistent Kinetostatic Indices for Planar 3-DOF Parallel Manipulators, Application to the Optimal Kinematic Inversion, *Proceedings of the ASME 2005 IDETC/CIE Conference*, 2005.

[5] Theingin, Chen, I.-M., Angeles, J. and Li, C., Management of parallel-manipulator singularities using joint-coupling *Advanced Robotics*, vol. 21, no. 5-6, pp. 583–600, 2007.

[6] Arakelian, V., Briot, S. and Glazunov, V., Increase of Singularity-Free Zones in the Workspace of Parallel Manipulators Using Mechanisms of Variable Structure. *Mechanism and Machine Theory*, 43(9), pp. 1129-1140, 2008.

[7] Rakotomanga, N., Chablat, D., Caro, S., Kinetostatic performance of a planar parallel mechanism with variable actuation, 11th International Symposium on Advances in Robot Kinematics, Kluwer Academic Publishers, Nantes, France, June, 2008

[8] Bonev, I. A., Gosselin, C. M., Singularity Loci of Planar Parallel Manipulators with Revolute Joints, Proc. 2nd Workshop on Computational Kinematics, Seoul, 2001.

[9] Chablat, D., Jha, R., Caro, S., A framework for the control of a parallel manipulator with several actuation modes. In Industrial Informatics (INDIN), IEEE 14th International Conference on (pp. 190-195), 2016.

[10] Caro, S., Chablat, D., Wenger, P., and Kong, X., Kinematic and dynamic modeling of a parallel manipulator with eight actuation modes. In New Trends in Medical and Service Robots (pp. 315-329). Springer, 2014.

[11] Takesue, N., Komoda, Y., Murayama, H., Fujiwara, K., and Fujimoto, H., Scissor lift with real-time self-adjustment ability based on variable gravity compensation mechanism. Advanced Robotics, 30(15), 1014-1026, 2016.

[12] Islam, M. T., Yin, C., Jian, S., and Rolland, L., Dynamic analysis of Scissor Lift mechanism through bond graph modeling, IEEE/ASME International Conference on Advanced Intelligent Mechatronics, 2014.

[13] Rolland, L., Kinematics Synthesis of a New Generation of Rapid Linear Actuators for High Velocity Robotics. In Advanced Strategies for Robot Manipulators. InTech, 2010.

[14] Siropa, Algebraic and robotic functions, http://siropa.gforge.inria.fr/doc/files/siropa-mpl.html, 2018.

[15] Jha, R., Chablat, D., Barin, L., Rouillier, F. and Moroz, G., Workspace, Joint space and Singularities of a family of Delta-Like Robot Mechanism and Machine Theory, Vol. 127, pp.73–95, September 2018.

[16] Collins, G. E., "Quantifier Elimination for Real Closed Fields by Cylindrical Algebraic Decomposition", Springer Verlag, 1975.

[17] Caro, S., Chablat, D. and Hu, Y., Algorithm for the Actuation Mode Selection of the Parallel Manipulator NAVARO ASME 2014 International Design Engineering Technical Conferences and Computers and Information in Engineering Conference, Buffalo, 2014.

Appendix

Actuation mode 1

$$-3(-30\sqrt{3}y+x^2+y^2+1800C_\alpha-90x-300)(C_\alpha-1/3)=0 \tag{20}$$

Actuation mode 2

$$\begin{aligned}((-240x+5400)yC_\alpha^2+((120x^2-120y^2-5400x)S_\alpha+360y(x-50))C_\alpha+\\ (360y^2+1800x)S_\alpha+120y(x+45))\sqrt{3}+(-120x^2+120y^2+16200x)C_\alpha^2+\\ ((-240x+16200)yS_\alpha+(-4x+180)y^2-\\ 4x^3+540x^2-18000x)C_\alpha-4y(x^2+y^2-90x+8550)S_\alpha-60x^2-180y^2-5400x=0\end{aligned} \tag{21}$$

Actuation mode 3

$$\begin{aligned}(-160y(x+45)C_\alpha^2+((80x^2-80y^2+7200x-648000)S_\alpha-4y(x^2+y^2-180x-600))C_\alpha+\\ (4x^3+4xy^2-720x^2+30000x+108000)S_\alpha+80y(x-90))\sqrt{3}+\\ (-240x^2+240y^2+21600x)C_\alpha^2+(-480y(x-45)S_\alpha-4(x-90)(x^2+y^2-180x-600))C_\alpha-\\ 4y(x^2+y^2-180x+7500)S_\alpha+120x^2-120y^2-21600x+972000=0\end{aligned} \tag{22}$$

Actuation mode 4

$$\begin{aligned}(-160y(x-135)C_\alpha^2+((80x^2-80y^2-21600x+648000)S_\alpha+4x^2y+4y^3-34800y)C_\alpha+\\ (-4x^3+360x^2+(-4y^2+2400)x+360y^2-108000)S_\alpha+80xy)\sqrt{3}+(240x^2-240y^2-21600x)C_\alpha^2+\\ (480y(x-45)S_\alpha-4x^3-4xy^2+34800x)C_\alpha+(-4x^2y-4y^3+2400y)S_\alpha-120x^2+120y^2=0\end{aligned} \tag{23}$$

Actuation mode 5

$$\begin{aligned}((1680xy-70200y)C_\alpha^2+((-840x^2+840y^2+70200x)S_\alpha-12x^2y-12y^3-2100y)C_\alpha+\\ (12x^3+12xy^2-95100x)S_\alpha-840xy+32400y)\sqrt{3}+(840x^2-840y^2-210600x+6804000)C_\alpha^2+\\ ((1680xy-210600y)S_\alpha-36x^3+3240x^2+(-36y^2-6300)x+3240y^2+1323000)C_\alpha-\\ 36y(x^2+y^2-7925)S_\alpha+180x^2+1020y^2+97200x-6902000=0\end{aligned} \tag{24}$$

Actuation mode 6

$$\begin{aligned}((80x^2-80y^2-7200x+324000)C_\alpha^2+(160y(x-45)S_\alpha+360y^2-54000)C_\alpha-\\ 360y(x-45)S_\alpha-60x^2+20y^2+5400x-156000)\sqrt{3}-\\ 4y(x^2+y^2-90x+8100)C_\alpha+4(x-45)(x^2+y^2-90x)S_\alpha+5400y=0\end{aligned} \tag{25}$$

Actuation mode 7

$$\begin{aligned}(480y(x-45)C_\alpha^2+((-240x^2+240y^2+21600x)S_\alpha+4y(x^2+y^2-180x+8100))C_\alpha-\\ 4(x-90)(x^2+y^2-180x)S_\alpha-240y(x-45))\sqrt{3}+(1944000-240x^2+240y^2-21600x)C_\alpha^2+\\ (-480y(x+45)S_\alpha-324000-12x^3+2160x^2+(-12y^2-97200)x)C_\alpha-12y(x^2+y^2-180x)S_\alpha-\\ 240y^2+32400x-936000=0\end{aligned} \tag{26}$$

Actuation mode 8

$$-S_\alpha(30\sqrt{3}y-x^2-y^2-1800C_\alpha+90x+300)=0 \tag{27}$$